New Asymmetric AB_n-Shaped Amphiphilic Poly(ethylene glycol)-*b*-[Poly(L-lactide)]$_n$ (n = 2, 4, 8) Bridged with Dendritic Ester Linkages: I. Syntheses and Their Characterization

Qiaobo Li,[†] Faxue Li,[†,‡] Lin Jia,[†] Yang Li,[†] Yanchun Liu,[†] Jianyong Yu,[‡] Qiang Fang,[†] and Amin Cao*[,†]

Laboratory for Polymer Materials, Shanghai Institute of Organic Chemistry, Chinese Academy of Sciences, 354 Fenglin Road, Shanghai 200032, China, and College of Textiles, Donghua University, 1882 Yan-an west Road, Shanghai 200051, China

Received April 18, 2006; Revised Manuscript Received May 12, 2006

This study presents new investigations on chemical syntheses and characterization of new asymmetric AB_n-shaped amphiphilic diblock methoxy poly(ethylene glycol)-*b*-[poly(L-lactide)]$_n$, MPEG-*b*-(PLLA)$_n$ (n = 2, 4, and 8), bridged with dendritic ester linkages. First, a new series of $A(OH)_n$-shaped hydroxy end-capped MPEG-$(OH)_2$, MPEG-$(OH)_4$, and MPEG-$(OH)_8$ bearing corresponding one- to three-generation dendritic ester moieties were efficiently derived from the starting MPEG (M_n = 2 KDa) and 2,2′-bis(hydroxymethyl)propionic acid (Bis-HMPA) via ester coupling and a facile hydroxy protection−deprotection cycle, and then, chemical structures of these functional MPEG-$(OH)_n$ were characterized by nuclear magnetic resonance spectrometry (NMR) and MALDI−FTMS. Subsequently, by employing these MPEG-$(OH)_n$ as functional macroinitiators, new asymmetric AB_n-shaped amphiphilic MPEG-*b*-$(PLLA)_2$ **S1**, MPEG-*b*-$(PLLA)_4$ **S2**, and MPEG-*b*-$(PLLA)_8$ **S3** bridged with dendritic Bis-HMPA ester linkages of **L1**−**L3** as well as linear structural MPEG-*b*-PLLA references (**R1**−**R3**) were synthesized through the $SnOct_2$-catalyzed ring-opening polymerization (ROP) of L-lactide at 130 °C in *m*-xylene solution, and their structures were further examined by NMR and gel permeation chromatography (GPC). It was demonstrated that the functional MPEG-$(OH)_n$ efficiently initiated the ROP of LLA, finally leading to successful formation of the AB_n-shaped amphiphilic MPEG-*b*-$(PLLA)_n$ (n = 2, 4, and 8) with each PLLA arm weight close to 2 KDa and very narrow molecular weight distribution. Moreover, thermal history, crystallization, and spherulite morphologies were studied by means of differential scanning calorimeter (DSC), thermal gravimetric analyzer (TGA), and polarized microscope (POM) for these new structural amphiphilic **S1**−**S3** as well as the linear **R1**−**R3**, intriguingly indicating a strong molecular architecture dependence of segmental crystallizability, spherulite morphology, and apparent crystal growth rate. Due to the favorable biodegradability and biocompatibility of the PLLA and MPEG, these results may therefore create new possibilities for these novel structural AB_n-shaped amphiphilic MPEG-*b*-$(PLLA)_n$ as potential biomaterials.

Introduction

Since self-assembly of asymmetric star-shaped copolymers with AB_2, AB_3, and AB_n block architectures has been known to possess unique characteristics during micellization and/or in the condensed state,[1,2] this category of new functional polymers has recently been intensively studied.[3−7] Asymmetric AB_2-shaped (here denoted as Y-shaped) block copolymers were reported to be routinely synthesized in a chemical strategy via living anionic or cationic polymerization.[1,2,8,9] In the past decade, recent advances in polymerization techniques allow more sophisticated approaches to nontraditional polymers bearing complicated architectures (grafted, star-shaped, mikto-armed, hyperbranched, dendritic).[10−12] For instance, Gnanou et al.[13] designed and prepared heteroarm Y-shaped polystyrene-*b*-[poly(ethylene oxide)]$_2$ PS-*b*-$(PEO)_2$ with a combination of anionic polymerization and group protection chemistry. New ABC-shaped functional polymers bearing three distinct arms were synthesized by combining three different controlled/living polymerization methodologies, namely, ring-opening polymerization (ROP), atom-transfer radical polymerization (ATRP), and nitroxide-mediated radical polymerization (NMRP).[14] Most recently, Armes et al.[15,16] reported a Y-shaped stimulus-responsive amphiphilic block copolymer with aid of monoamine-capped poly(alkylene oxide)s and ATRP, and structurally well-defined Y-shaped zwitterionic poly(2-diethylamino ethyl methacrylate)-*b*-[poly(succinyloxyethyl methacrylate)]$_2$ PDEA-*b*-$(PSEMA)_2$ were further synthesized. In addition, Gnanou et al.[17] combined an ATRP strategy and a multistep preparation route to synthesize a Y-shaped polystyrene-*b*-[poly(*tert*-butyl acrylate)]$_2$ PS-*b*-$(P^tBA)_2$, and new series of mikto-armed amphiphilic polystyrene-*b*-[poly(acrylic acid)]$_2$ PS-*b*-$(PAA)_2$ and polystyrene-*b*-[poly(glutamic acid)]$_2$ PS-*b*-$(PGA)_2$ were interestingly found to be water-soluble and stimuli-responsive.[18]

Regarding the macromolecular architecture dependence of self-assembled structures and their properties, morphological behavior has been predicted by Milner[19,20] for new A_mB_n-shaped block copolymers bearing individual A_2B,[21] A_3B,[22] A_5B,[23] A_nB_n,[24] and multigrafted architectures. The aggregation number and overall size of AB_3-shaped diblock PS-*b*-$(PI)_3$ micelles self-assembled in selective solvent were found to be smaller than those of corresponding linear structural diblock counterparts.[25] As for the amphiphilic star-shaped AB_m diblock copolymer of

* Author for correspondence. Tel: +86-21-54925303. Fax: +86-21-64166128. Email: acao@mail.sioc.ac.cn.
† Chinese Academy of Sciences.
‡ Donghua University.

10.1021/bm060372l CCC: $33.50
Published on Web 07/08/2006

PEO-*b*-$(PS)_m$,[26−28] their molecule self-assembly and surface morphology have been investigated to organize interesting well-ordered curved interfaces and microscopic domain structures.

On the other hand, biodegradable polymers have nowadays been attracting great interest in both fundamental research and industrial applications. Among them, synthetic poly(L-lactide) (PLLA), which could be derived from renewable biomass, was focused on for its important biomedical applications and as a sound candidate for ecological plastics due to its favorable resorbability in vivo and its biodegradability.[29−33] Furthermore, hydrophilic poly(ethylene glycol) (PEG) has also been recognized as a water-soluble biocompatible polymer or building block with important biological and pharmaceutical applications.[34] With the advantages of PLLA and poly(ethylene glycol), a number of diblock methoxy poly(ethylene glycol)-*b*-poly(L-lactide)s (MPEG-*b*-PLLA) have been synthesized,[35] and their morphologies, crystallization behavior, and biomedical applications were thereby investigated.[36,37] Because the architecture of block structural functional polymers would play very important roles in the self-assembled interfaces and microscopic domains, new asymmetric AB_n-shaped amphiphilic diblock copolymers bearing hydrophilic PEG (A) and hydrophobic PLLA arms (B_n) seem interesting for self-assembly of new functional hierarchies.

In this study, a series of new AB_n-shaped (AB_2, AB_4, and AB_8) biodegradable amphiphilic methoxy poly(ethylene glycol)-*b*-[poly(L-lactide)]$_n$ MPEG-*b*-$(PLLA)_n$ have been rationally designed and synthesized with dendritic polyester linkages (**L1**, **L2**, and **L3**). Subsequently, their chemical structures were characterized by NMR, MALDI−FTMS, and GPC. Finally, a molecular architecture dependence of thermal and crystallization behavior and spherulitic morphologies was studied and will be carefully discussed.

Experimental Section

Materials. 2,2′-Bis(hydroxymethyl)propionic acid (Bis-HMPA) (AR grade) was purchased from Tokyo Kasei Ltd., Japan. 2,2′-Dimethoxy propane (98%) was commercially supplied by Lancaster. Reagents of 4-dimethylamino pyridine (DMAP) (99%) and methoxy poly(ethylene glycol) MPEG-2K (M_n = 2 KDa) were received from Aldrich Chemical, and the MPEG-2K was dissolved in CH_2Cl_2, then precipitated in dried ethyl ether and dried over P_2O_5 under vacuum prior to use. Monomer of L-lactide was kindly provided by X. Pan of Synica Chemical Ltd., China, and was further purified four times via recrystallization in ethyl acetate. Stannous octanoate from Aldrich Chemical was distilled under reduced pressure and then dissolved in dry toluene before use. In addition, solvents of toluene and *m*-xylene were distilled with metallic sodium and benzophenone, and all the other reagents of analytical grade were used as received.

Preparation of the A-$(OH)_n$-Shaped MPEG-$(OH)_n$ Macroinitiators (n = 2, 4, and 8). For the sake of preparing new amphiphilic AB_n-shaped diblock MPEG-*b*-$(PLLA)_n$, the hydroxy end-capped macroinitiators of MPEG-$(OH)_n$ (n = 2, 4, and 8) were first synthesized with corresponding dendritic Bis-HMPA ester linkages (**L1**, **L2**, and **L3**). For instance, a MPEG-$(OH)_2$ (n = 2) was synthesized via a three-step strategy as shown in Scheme 1.

Synthesis of Isopropylidene-2,2′-bis(methoxyl) Propionic Acid. At first, compound **1** of isopropylidene-2,2′-bis(methoxyl) propionic acid was synthesized as partially described in the literature.[39,40] Bis-HMPA (10 g, 74.55 mmol), 2,2′-dimethoxypropane (13.8 mL, 111.83 mmol), and *p*-toluenesulfonic acid monohydrate (0.71 g, 3.73 mmol) were in turn dissolved in 50 mL of acetone, and then, the mixture was stirred at room temperature for 2 h. After neutralization of the residual *p*-toluenesulfonic acid by adding about 5 mL of NaOH methanol solution (0.16 g), the solvent was evaporated at room temperature. The residual mass was again dissolved in 250 mL of CH_2Cl_2 and was further extracted twice with 20 mL of distilled water. Then, the organic phase was collected and dried over anhydrous $MgSO_4$ and evaporated to give a final white crystal product **1** with a yield of 77%.

Scheme 1. Chemical Preparation of New AB_2-Shaped MPEG-*b*-$(PLLA)_2$ with Linkage **L1**

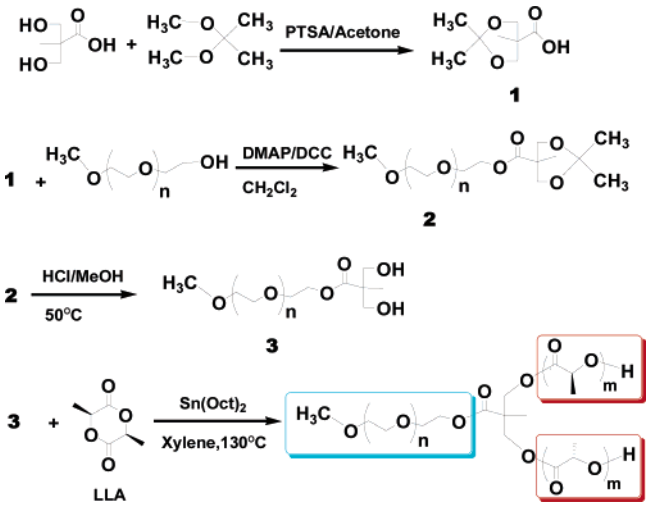

^{1}H NMR ($CDCl_3$, in ppm) 1.21 (s, 3H, C*H*$_3$), 1.44 (dd, 6H, C*H*$_3$), 3.71 (d, 2H, C*H*$_2$), 4.21 (d, 2H, C*H*$_2$).

Preparation of Hydroxy-Protected MPEG-$(OH)_2$ Synthetic Precursor with First-Generation Dendritic Ester Linkage. Starting MPEG-2K (20.0 g, 10 mmol), 2.61 g of the above-synthesized compound **1** (15 mol,1.5 equiv), *N*,*N*′-dicyclohexylcarbodiimide (DCC) (3.4 g,16.5 mmol,1.65 equiv), DMAP (372 mg, 3 mmol, 0.2 equiv), and 150 mL of CH_2Cl_2 were placed into a 250-mL one-necked round-bottom flask, and the reaction mixture was stirred at ambient temperature for 36 h. Afterward, the reaction mixture was filtered to remove insoluble mass and further concentrate the filtrate to 40 mL. Finally, the mixture was precipitated in ethyl ether, and the collected solid product **2** was dried in a vacuum oven with a yield of 97%.

*Synthesis of New MPEG-$(OH)_2$ Macroinitiator with First-Generation Dendritic Ester Linkage **L1**.* Ten grams of the above obtained product **2** (5 mmol) was dissolved in 100 mL of methanol, and then, 10 mL of 1 M HCL was added into the mixture solution, and the mixture kept stirring at 50 °C for 6 h. When the reaction completed, the mixture was evaporated under reduced pressure to remove the solvent. The obtained solid product was further dissolved in 200 mL of $CHCl_3$ and dried with anhydrous $MgSO_4$ overnight. Finally, the reaction mixture was filtered and concentrated to 40 mL and then precipitated in dry ethyl ether. The resulting solid product **3** was further dried over P_2O_5 under vacuum with a yield of 65%.

In a similar way, new A-$(OH)_n$-shaped MPEG-$(OH)_n$ macroinitiators (n = 4 and 8) were prepared with corresponding two- and three-generation dendritic Bis-HMPA ester linkages of **L2** (yield: 62%) and **L3** (yield: 57%).

Synthesis of New AB_n-Shaped MPEG-b-$(PLLA)_2$, MPEG-b-$(PLLA)_4$, and MPEG-b-$(PLLA)_8$. With the prepared MPEG-$(OH)_2$ **3** as a macroinitiator, new AB_2-shaped amphiphilic diblock MPEG-*b*-$(PLLA)_2$ was synthesized through ring-opening polymerization of L-lactide in a Schlenk tube with stannous octanoate catalyst. First, a flame-dried flask containing 0.5 g of MPEG-$(OH)_2$ **3** macroinitiator (0.25 mmol) and 1.0 g of L-lactide (6.94 mmol) was purged with dry N_2, and then, 0.3 mL of the $SnOct_2$ toluene solution (46 mg/mL) and 5 mL of *m*-xylene were added. Subsequently, this reaction mixture was allowed to heat up to 130 °C and kept stirring for 48 h. When the reaction completed (tracked by ^{1}H NMR), the mixture was cooled to ambient temperature and precipitated in an excess amount of ethyl ether; the collected precipitates were washed several times with ethyl ether and then dried

Scheme 2. New AB$_n$-Shaped Asymmetric Amphiphilic MPEG-*b*-(PLLA) $_n$ (n = 2, 4, 8) Bridged with Dendritic Bis-MPA Ester Linkages **L1**, **L2**, and **L3**

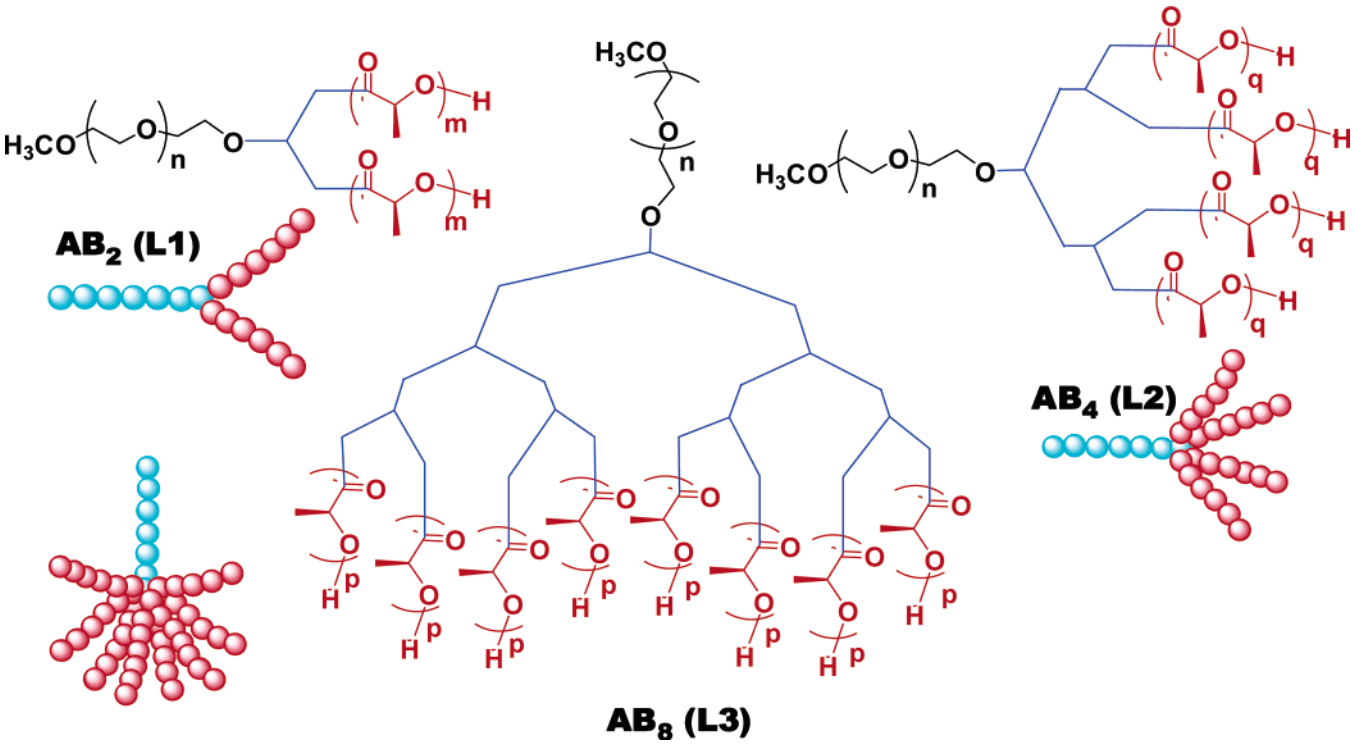

under vacuum. As a result, new AB$_2$-shaped amphiphilic MPEG-*b*-(PLLA)$_2$ denoted sample **S1** was obtained.

^{1}H NMR ($CDCl_3$, in ppm) 5.20 (q, >C*H*-OCO), 3.60 (d, −OCH_2CH_2O-), 1.50 (s, −CH_3). In the same strategy, two new AB$_4$- and AB$_8$-shaped amphiphilic copolymers MPEG-*b*-(PLLA)$_4$ (**S2**) and MPEG-*b*-(PLLA)$_8$ (**S3**) were initiated with corresponding MPEG-(OH)$_4$ and MPEG-(OH)$_8$, and these block copolymers (**S2**−**S3**) were prepared with PLLA arm lengths similar to those of **S1** via tuning the initial LLA monomer to macroinitiator feeding molar ratios.

Additionally, to clarify the polymer architecture dependence of physical properties, linear structural amphiphilic diblock MPEG-*b*-PLLA references denoted **R1**−**R3** bearing similar PLLA component compositions were also synthesized through ring-opening polymerization of L-lactide with the starting MPEG-2K and $SnOct_2$ catalyst.

Characterization Procedures. *GPC Characterization.* Molecular weights of the synthesized AB$_n$-shaped MPEG-*b*-(PLLA)$_n$ as well as their linear structural counterparts were measured under 40 °C on a Perkin-Elmer 200 Series gel permeation chromatograph equipped with a refractive index detector (RI) and a network chromatography interface NCI 900. Double PLgel 5-μm mixed-D type GPC columns (300 × 7.5 mm, Polymer Laboratories Ltd., U.K.) were employed in a series with chloroform as the eluent at a flow rate of 1.0 mL/min. A commercial calibration kit of polystyrene standards (Showa Denko Ltd., Japan) was utilized to calibrate the GPC elution traces. As a result, the molecular weights (M_w, M_n) and their distributions were thus evaluated.

^{1}H and ^{13}C NMR. Measurements of NMR spectra were conducted under ambient temperature in $CDCl_3$ on a Bruker AMX300 spectrometer and Varian VXR 300 Fourier transform NMR spectrometer operating at 300.0 and 75.5 MHz for the corresponding ^{1}H and ^{13}C nuclei, respectively. Tetramethylsilane (TMS) was hereby employed as the internal chemical shift reference.

Mass Spectra. Structural characterization of starting MPEG-2K and its hydroxy end-capped derivative MPEG-(OH)$_n$ bearing various dendritic ester linkages was conducted on an IonSpec MALDI 4.70 T-FTMS system with N_2 laser beam (λ = 337 nm) and a mass scanning range of 400−3000 m/z.

Thermal Analysis. Thermal properties were characterized on a Perkin-Elmer Pyris 1 differential scanning calorimeter (DSC) and a thermal gravimetrical analyzer (TGA). First, 2.0−3.0 mg of a synthesized polymer sample was sealed in an aluminum pan and then the sample heated from ambient temperature to 170 °C at 20 °C/min (first heating run). Melting point (T_m) and enthalpy of fusion (ΔH_m) were evaluated as the melting peak top temperature and the integral of endothermic traces, respectively. Subsequently, the sample melt at 170 °C for 1 min was cooled to 0 °C at a cooling rate of 20 °C /min (cooling run), and the crystallization temperature (T_c) of each crystallizable block component was evaluated as the peak top temperature of the exothermic trace. In addition, TGA analyses (TGA) were implemented from 50 to 450 °C at 20 °C/min under flowing nitrogen atmosphere (45 mL/min). Weight loss profiles were employed to evaluate individual block component composition, and peak top temperatures (T_d) of the dTGA trace were evaluated to assess thermal stability for each block component.

Polarized Microscope (POM). Spherulite morphologies and isothermal growth rates were characterized under various crystallization temperatures for the linear MPEG-*b*-PLLA and new AB$_n$-shaped MPEG-*b*-(PLLA)$_n$ samples on an Olympus BX51 polarized microscope with an attached hot stage. First, a synthesized MPEG-*b*-(PLLA)$_n$ sample was sandwiched between two thin glass cover slides. Subsequently, the sample was allowed to heat up over their corresponding melting temperatures and further kept for 1 min. Finally, the sample temperature was rapidly decreased to a predetermined isothermal crystallization temperature for crystallization kinetic and spherulite morphological studies.

Results and Discussion

As a general approach to new AB$_n$-shaped asymmetric amphiphilic diblock MPEG-*b*-(PLLA)$_n$, chemical synthesis of an AB$_2$-shaped MPEG-*b*-(PLLA)$_2$ is illustrated in Scheme 1. Since Bis-HMPA has been widely applied as one of the most important biocompatible building blocks to construct dendritic degradable polyesters with abundant favorable hydroxy-terminal functional groups,[42−46] the macroinitiators of MPEG-(OH)$_n$ with n hydroxy end groups were therefore designed and were

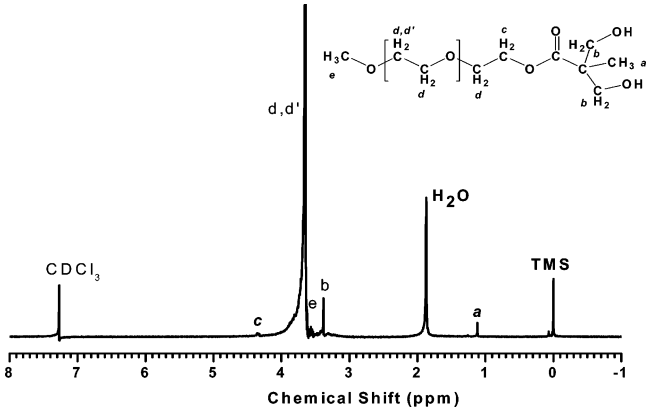

Figure 1. ^{1}H NMR spectrum of the hydroxy-deprotected macroinitiator of MPEG2K−$(OH)_2$.

synthesized with one- to three-generation dendritic Bis-HMPA ester linkages **L1**−**L3**, and a new series of the AB_n-shaped amphiphilic MPEG-*b*-$(PLLA)_n$ with well-defined structures as shown in Scheme 2 were further prepared with a successive $SnOct_2$ catalyzed ring-opening polymerization of L-lactide.

Chemical Synthesis of Functional MPEG-$(OH)_n$ Macroinitiators. Typically, the hydroxy-terminated MPEG-$(OH)_2$ comprising hydrophilic methoxy poly(ethylene glycol) MPEG with number average molecular weight equal to 2.0 KDa and a first generation of dendritic Bis-HMPA ester was prepared via coupling the hydroxy group of a MPEG and the carboxylic group of a hydroxy-protected Bis-MPA and a successive hydroxy functional group deprotection.[41,43,47] To characterize the molecular structures of synthesized MPEG-$(OH)_n$ bearing different dendritic ester linkages of **L1**−**L3**, ^{1}H NMR spectra were measured for the hydroxy-protected and hydroxy-deprotected MPEG-$(OH)_n$, as well as their starting MPEG-2K. As for the MPEG-$(OH)_2$ synthesis, a new occurrence of proton resonance at 4.30 ppm indicated a successful coupling between the carboxylic group of acetonide-protected Bis-HMPA and a hydroxy group of a MPEG-2K. Meanwhile, new additional proton resonances at 3.40 and 1.10 ppm could be assigned to corresponding methylene and methyl proton nuclei of the Bis-HMPA moiety. After the **L1** hydroxy deprotection, characteristic proton resonance at 1.43−1.46 ppm originated from the acetonide protection moiety entirely disappearing, and this demonstrated a complete deprotection of the terminal hydroxy groups and successful preparation of functional dihydroxy MPEG-$(OH)_2$ as shown in Figure 1.[41] Furthermore, Figure 2 depicts the ^{13}C NMR spectrum for the deprotected dihydroxy MPEG-$(OH)_2$ with a first-generation dendritic ester linkage **L1**. As compared with the starting MPEG-2K, new ^{13}C resonance signals could be observed at 17.8, 50.3, 62.2, 63.9, 67.5, and 176.1 ppm for the dihydroxy MPEG-$(OH)_2$, and these resonance signals could be assigned to ^{13}C nuclei of methyl, *tert*-butyl, methylene, and carbonyl of the Bis-HMPA moiety of the prepared MPEG-$(OH)_2$. The disappearance of a characteristic resonance around 20−25 ppm attributed to the acetonide moiety could further imply a complete deprotection of terminal hydroxy functional groups for the MPEG-$(OH)_2$ product.[41] In a similar characterization, ^{1}H and ^{13}C NMR spectra also confirmed the successful formation of functional MPEG-$(OH)_n$ bearing dendritic linkages **L2**−**L3** of two to three generation and four to eight hydroxy terminal groups.

To further shed new light on the molecular structures of the prepared functional MPEG-$(OH)_n$, their MALDI−FTMS were measured. Figure 3 shows the MALDI−FTMS for the starting MPEG-2K (Figure 3a) and corresponding dihydroxy MPEG-

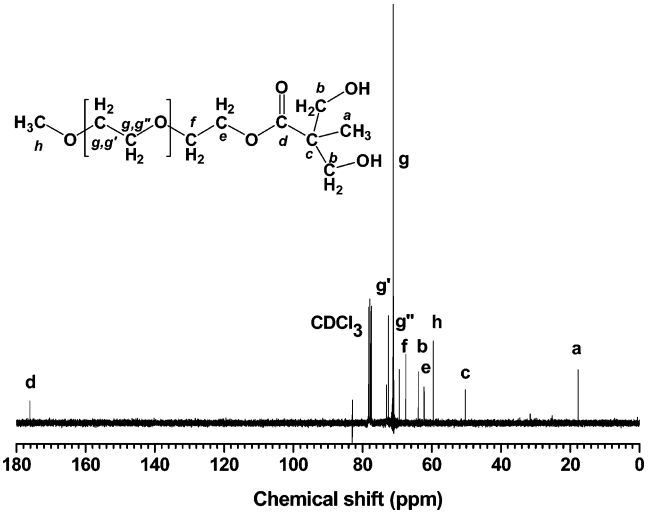

Figure 2. ^{13}C NMR spectrum of the hydroxy-deprotected macroinitiator of MPEG2K−$(OH)_2$.

$(OH)_2$ (Figure 3b). It was seen that the main mass spectral signals occurring at 1860, 1903, 1947, 1991, 2036, 2124, and 2168 *m*/*z* could be assigned to the Na^+ ionized species of $CH_3O(CH_2CH_2O)_mOH$ with corresponding degree of polymerization (*m*) equal to 41, 42, 43, 44, 45, 47, and 48, respectively. This indicates a narrow molecular weight distribution of the monofunctional starting MPEG-2K. In contrast, MALDI−FTMS of the synthesized MPEG-$(OH)_2$ exhibited a series of mass spectral signals at 2021, 2065, 2153, 2197, 2285, and 2330 *m*/*z*, and these signals could further be attributed to the Na^+ ionized macromolecular species bearing corresponding *m* values equal to 42, 43, 45, 46, 48, and 49, respectively. Moreover, a new series of the K^+ ionized MPEG-$(OH)_2$ species at 2037, 2125, 2169, 2213, 2257, and 2301 *m*/*z* were concurrently observed in Figure 3b. Furthermore, with respect to the synthesized MPEG-$(OH)_4$ bearing dendritic linkage **L2**, new characteristic MALDI−FTMS signals at 2211, 2255, 2299, 2343, 2388, 2432, 2475, and 2519 *m*/*z* were detected and could reasonably be assigned to the corresponding Na^+ ionized species with *m* values equal to 41, 42, 43, 44, 45, 46, 47, and 48. In contrast, MALDI−FTMS of the prepared MPEG-$(OH)_8$ with dendritic linkage **L3** exhibited a distinct series of mass spectral signals at 2692, 2736, 2780, and 2824 *m*/*z*, which could further be attributed to the H^+ ionized species with *m* values equal to 41, 42, 43, and 44, respectively. Therefore, this evidence quantitatively demonstrated successful syntheses of new hydroxy end-capped functional MPEG-$(OH)_n$ (n = 2, 4, 8) with diverse dendritic Bis-HMPA linkages.

Syntheses of Asymmetric Amphiphilic Diblock MPEG-*b*-$(PLLA)_n$ (n = 2, 4, 8). Up to the present date, aliphatic poly(L-lactide) seems to be an important biodegradable polyester and/or an ideal lipophilic building block to construct a wide variety of biodegradable amphiphilies, and thus, it has been intensively investigated in functional biological vectors and biomimetic systems.[29−33] In general, the poly(L-lactide) was routinely synthesized through ring-opening polymerization of enantiopure L-lactide monomer under a catalyst of alkylmetal or metal alkoxide with an alcohol initiator,[35,38,48,53] and linear structural amphiphilic MPEG-*b*-PLLA and PLLA-*b*-PEG-*b*-PLLA had been extensively studied.[35] In our pervious study, the ROP of L-lactide under 130 °C and a $SnOct_2$ catalyst seemed to be better in *m*-xylene solution for preparation of more structurally perfect star-shaped PLLA products.[38] Therefore, in this work, new AB_n-shaped diblock MPEG-*b*-$(PLLA)_n$ were synthesized under 130 °C via the $SnOct_2$ catalyzed ROP of

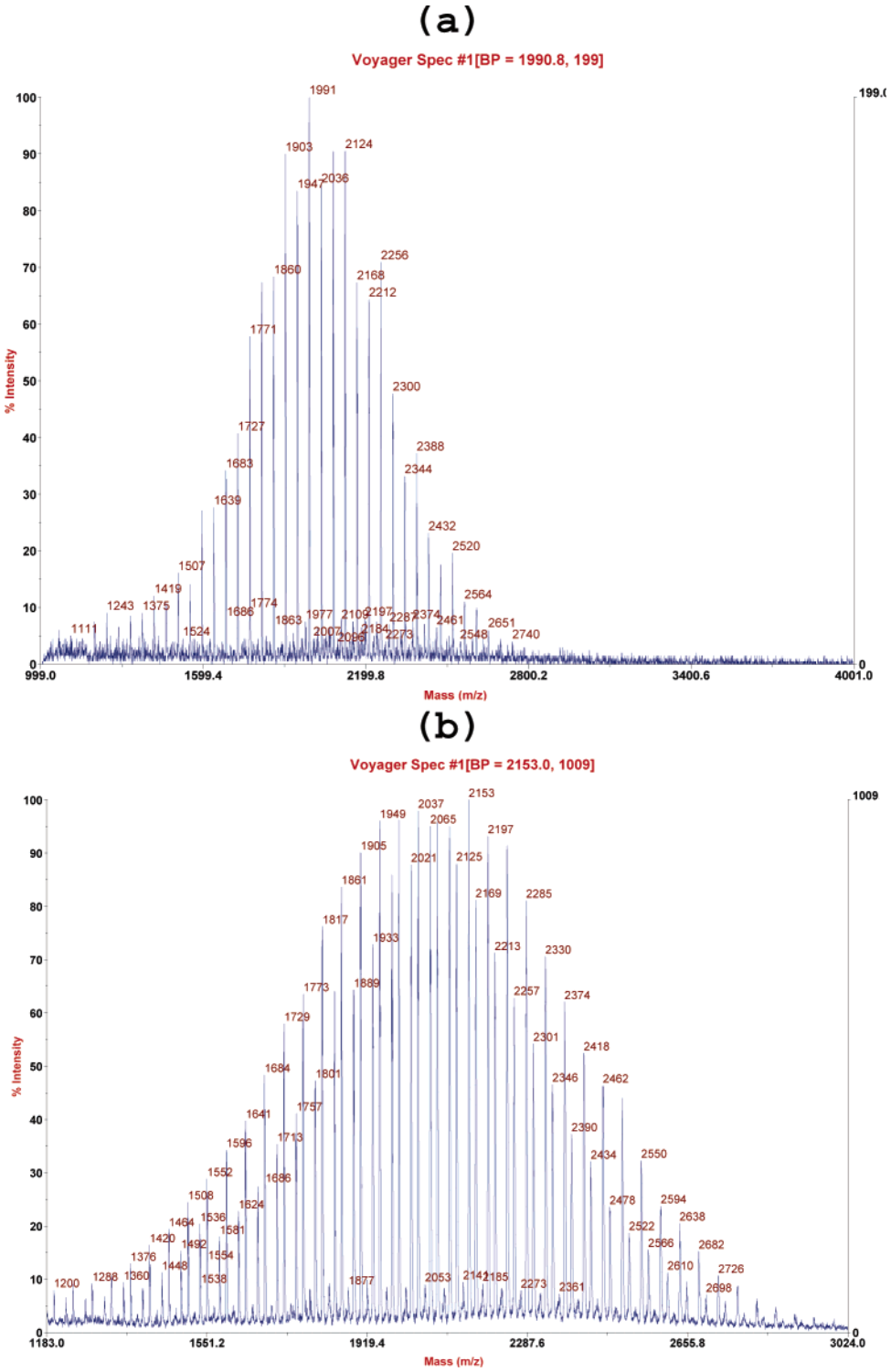

Figure 3. MALDI-TOF mass spectra of (a) the starting MPEG-2K and (b) the resulted MPEG2K−$(OH)_2$ derivative.

L-lactide with corresponding MPEG-$(OH)_n$ macroinitiators (n = 2, 4, 8) in *m*-xylene solution.

Figure 4 shows GPC elution traces for the synthesized dihydroxy MPEG-$(OH)_2$ macroinitiator (a), new MPEG-*b*-$(PLLA)_2$ (b), MPEG-*b*-$(PLLA)_4$ (c), and MPEG-*b*-$(PLLA)_8$ products (d) with designed molecular weight of PLLA arms close to 2 KDa, regardless of their different architectures. It was found that either a MPEG-$(OH)_2$ macroinitiator or a prepared new MPEG-*b*-$(PLLA)_n$ exhibited a much narrower symmetric GPC elution trace, implying an efficient initiation of the hydroxy end-capped MPEG-$(OH)_n$. After the copolymerization of the PLLA arm, GPC elution traces for the new diblock MPEG-*b*-$(PLLA)_n$ obviously shifted toward the high molecular weight region, and more arms (n) of a prepared MPEG-*b*-$(PLLA)_n$ finally led to an apparent higher molecular weight of the achieved product. Alternatively, ^{1}H NMR spectrum of the synthesized diblock MPEG-*b*-$(PLLA)_2$ concurrently exhibited characteristic resonances around 3.60−3.70 and 5.20 ppm, which could be attributed to the methylene proton of $-CH_2CH_2O-$ of the MPEG block and the methine proton of $-O-CH(CH_3)-CO-$ of the lactide building blocks. Furthermore, the EG/LA comonomer molar ratios of the synthesized diblock copolymers were evaluated,[35] and number average molecular weights denoted $M_{n,NMR}$ could be calculated in

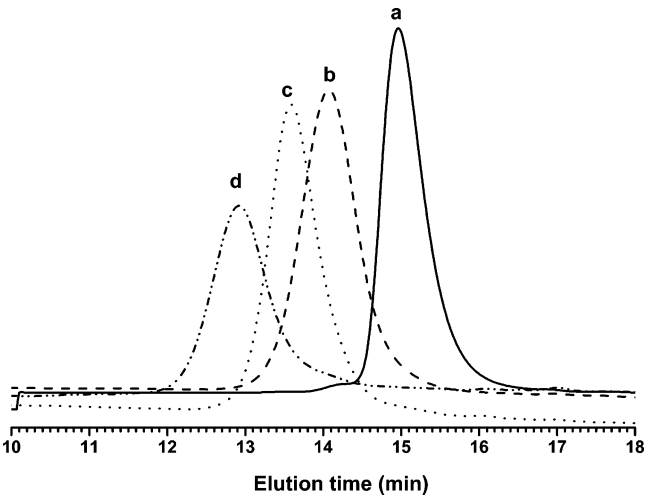

Figure 4. GPC traces for the macroinitiator and new AB_n-shaped polymers: (a) dihydroxy MPEG-$(OH)_2$; (b) AB_2-shaped MPEG-*b*-$(PLLA)_2$; (c) AB_4-shaped MPEG-*b*-$(PLLA)_4$; (d) AB_8-shaped MPEG-*b*-$(PLLA)_8$.

accordance with eqs 1 and 2

$$M_{n,NMR} = DP_{MPEG} \times 44 + DP_{PLLA} \times 144 \quad (1)$$

$$DP_{PLLA} = 2 \times DP_{PEG} \times (I_{5.20}/I_{3.65}) \quad (2)$$

Where DP_{MPEG} and DP_{PLLA} indicate the degree of polymerization for individual MPEG and PLLA block; $I_{3.65}$ and $I_{5.20}$ denote the integral resonance intensities at 3.65 and 5.20 ppm attributed to the MPEG and PLLA comonomers, respectively.

Table 1 summarizes synthetic results for the new AB_n-shaped amphiphilic MPEG-*b*-$(PLLA)_2$ **S1**, MPEG-*b*-$(PLLA)_4$ **S2**, and MPEG-*b*-$(PLLA)_8$ **S3** bearing a MPEG-2K block and multiple PLLA arms (each arm designed to be 2 KDa). In the meantime, linear structural MPEG-*b*-PLLA **R1**, **R2**, and **R3** were simultaneously prepared with similar PLLA compositions to the **S1**, **S2**, and **S3**. It was seen that after a polymerization time of 48 h both branched **S** and linear **R** series of diblock amphiphilic copolymers were prepared with LLA monomer conversions higher than 95%, and narrow molecular weight distribution equal to 1.10−1.20 were achieved, indicating uniform and well-controlled molecular architectures of the linear and new AB_n-shaped MPEG-*b*-$(PLLA)_n$. It was also noteworthy that the GPC molecular weights of the linear reference diblock MPEG-*b*-PLLA (**R1**, **R2**, and **R3**) tended to be lower than those values evaluated by ^{1}H NMR, while a different tendency in molecular weights could be observed for the AB_n-shaped asymmetric MPEG-*b*-$(PLLA)_n$ (**S1**, **S2**, and **S3**), and this result might be accounted for by two possible factors: (i) The molecular architecture would influence apparent molecular weights evaluated by size exclusion chromatography as often reported.[38] (ii) During the preparation of new MPEG-$(OH)_n$ macroinitiators, some components bearing different degrees of polymerization (m) for the MPEG would be lost as evidenced by MALDI−FTMS, and this would decrease the fraction of macroinitiator, thus leading to a LA/EG comonomer ratio higher than the theoretical value for the **S3**.

Thermal Characterization. Figure 5 depicts DSC traces recorded by the first heating scan for new AB_n-shaped diblock MPEG-*b*-$(PLLA)_n$ **S1**, **S2**, and **S3** as well as corresponding linear references **R1**, **R2**, and **R3**. It seems that only the MPEG-*b*-$(PLLA)_2$ **S1** and MPEG-*b*-PLLA **R1** with low PLLA weight fractions exhibited two endothermic peaks respectively attributed to crystal melting of the MPEG and PLLA blocks, and much narrower endothermic peaks and relatively high melting points (T_m) were apparently detected for the linear counterpart **R1**. This could be interpreted due to the architecture of two shortened PLLA arms for the synthesized MPEG-*b*-$(PLLA)_2$ **S1**. When increasing the PLLA weight fractions of the diblock **R** and **S** samples, increased melting points could be observed for the linear MPEG-*b*-PLLA due to the capability of their extended

Table 1. Synthetic Results for New AB_n-Shaped Diblock Amphiphilic Biodegradable MPEG-*b*-$(PLLA)_n$ (n = 2, 4, 8)

sample	LLA feeding molar ratio [-CH_2CH_2O-]/[LA]	LLA conversion[a] (%)	$M_{n,theor}$[b] (KDa)	$M_{n,GPC}$[c] (KDa)	$M_{n,NMR}$[d] (KDa)	M_w/M_n[c]	[-CH_2CH_2O-]/[LA] comonomer molar ratio in copolymers[d]	PLLA in copolymers[e] (wt %)
S1	1:0.61	98	5.9	7.5	5.8	1.15	1:0.53	63.6
S2	1:1.22	96	9.7	12.2	9.6	1.13	1:1.19	79.6
S3	1:2.44	97	17.7	24.8	17.5	1.16	1:2.64	88.8
R1	1:0.61	95	5.8	5.8	5.7	1.22	1:0.44	58.6
R2	1:1.22	95	9.6	7.1	9.5	1.17	1:0.95	73.7
R3	1:2.44	98	17.8	12.1	17.6	1.10	1:2.25	86.0

[a] LLA monomer conversions were evaluated by ^{1}H NMR. [b] Theoretical molecular weights were calculated by a sum of MPEG and PLLA blocks and the dendritic ester linkages. [c] Molecular weights were determined by GPC with polystyrene standards. [d] Molecular weights and comonomer molar ratios were evaluated by ^{1}H NMR. [e] PLLA block weight percentages were measured by TGA.

Table 2. Thermal Properties for the New AB_n-Shaped Diblock Amphiphilic Biodegradable MPEG-*b*-$(PLLA)_n$ (n = 2, 4, 8)

	MPEG block				PLLA block			
sample	T_m[a] (°C)	ΔH_m[a] (J/g)	T_c[a] (°C)	T_d[b] (°C)	T_m[a] (°C)	ΔH_m[a] (J/g)	T_c[a] (°C)	T_d[b] (°C)
S1	29.1	62.6	−8.5	391.4	127.3	37.1	71.0	285.2
S2	n.d.[c]	n.d.[c]	n.d.[c]	399.5	130.2	49.6	69.1	255.1
S3	n.d.[c]	n.d.[c]	n.d.[c]	390.2	138.8	29.1	75.0	260.4
R1	40.4	54.3	17.6	411.9	136.5	42.8	88.0	258.7
R2	40.0	11.4	n.d.[c]	412.3	142.8	49.0	87.8	261.7
R3	n.d.[c]	n.d.[c]	n.d.[c]	411.5	150.0	64.7	97.8	296.7
MPEG-2K[d]	47.8	187.2	32.3					
PLLA-8K[d]					147.7	60.6	110	

[a] Melting points, crystallization temperatures, and heat of fusion for individual block component were measured by DSC. [b] Thermal degradation temperatures were evaluated by TGA. [c] Not detected. [d] MPEG-2K and linear PLLA-8K expresses the references.

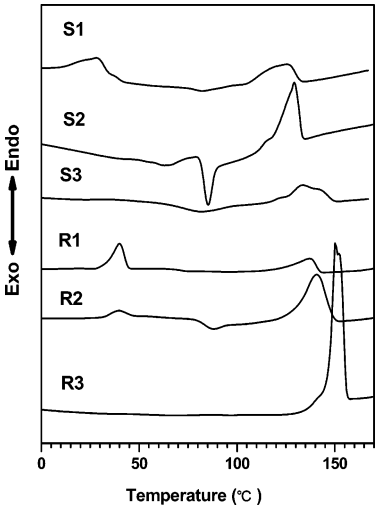

Figure 5. DSC traces by the first heating scan for the prepared AB$_n$-shaped amphiphilic MPEG-*b*-(PLLA)$_n$.

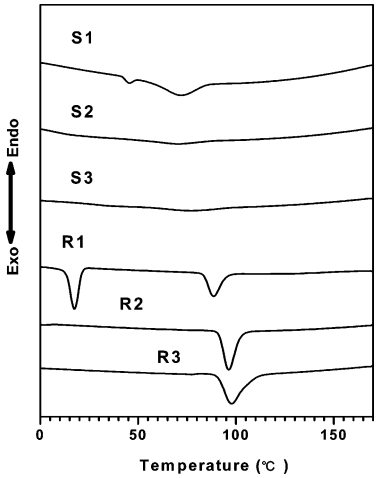

Figure 6. DSC traces by the cooling scan for the prepared AB$_n$-shaped amphiphilic MPEG-*b*-(PLLA)$_n$.

PLLA arms to fold thicker crystal lamella,[52] and during the heating scan, cold crystallization was obviously detected for the new MPEG-*b*-(PLLA)$_4$ **S2** and MPEG-*b*-PLLA **R2**. For the MPEG-*b*-(PLLA)$_8$ **S3** bearing eight PLLA arms bridged with a dendritic linkage **L3**, low chain/segmental crystallizabilities of both MPEG and PLLA blocks could be found even though the **S3** and **R3** have similar overall PLLA weight fractions higher than 85 wt %. This clearly demonstrated a strong macromolecular architecture dependence of crystallizability for the new AB$_n$-shaped MPEG-*b*-(PLLA)$_n$. Furthermore, Figure 6 depicts DSC thermal diagrams measured by the first cooling scan for the prepared AB$_n$-shaped amphiphilic MPEG-*b*-(PLLA)$_n$ (**S1**, **S2**, and **S3**) as well as the linear MPEG-*b*-PLLA references (**R1**, **R2**, and **R3**). It was found that linear diblock MPEG-*b*-PLLA **R1**, **R2**, and **R3** exhibited crystallization peak temperatures (T_c) around 95 °C for the PLLA block, and crystallization of the MPEG block could only be observed for the linear MPEG-*b*-PLLA **R1** with a high EG to LA comonomer molar ratio equal to 1/0.44. In contrast, very slow and weak crystallization could be detected for the AB$_n$-shaped amphiphilic MPEG-*b*-(PLLA)$_n$ (**S2** and **S3**), indicating a significantly depressed chain and/or segmental crystallizability due to possible densely packed multiarmed architectures as ever revealed for the three- to six-armed star-shaped PLLA.[38]

Figure 7 presents thermal degradation profiles for the new amphiphilic biodegradable MPEG-*b*-(PLLA)$_n$. Two weight-loss

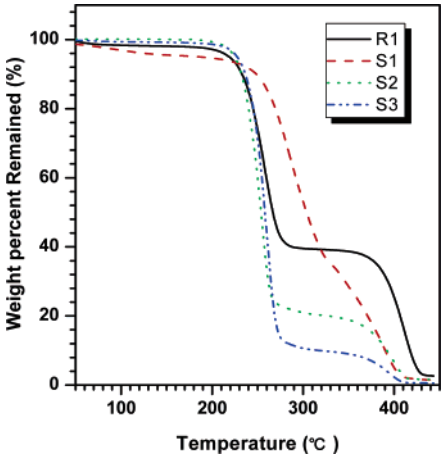

Figure 7. TGA profiles for the prepared AB$_n$-shaped amphiphilic MPEG-*b*-(PLLA).

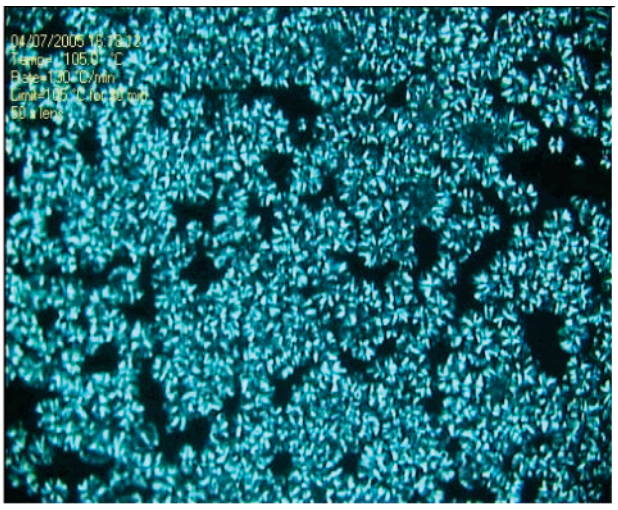

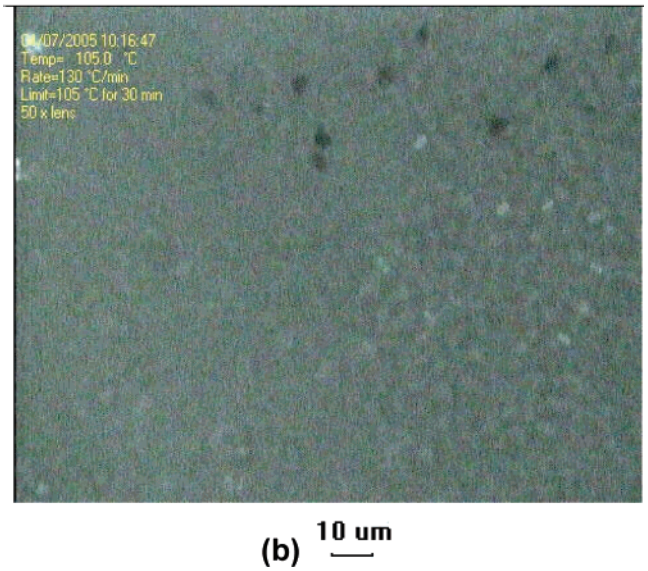

Figure 8. Spherulitic morphologies after 1-min isothermal crystallization at 105 °C for the samples bearing different architectures: (a) **R1**; (b) **S1**.

stages were typically observed, and the component degraded in a temperature range from 250 to 300 °C was attributed to the PLLA block, while the block of MPEG showed higher

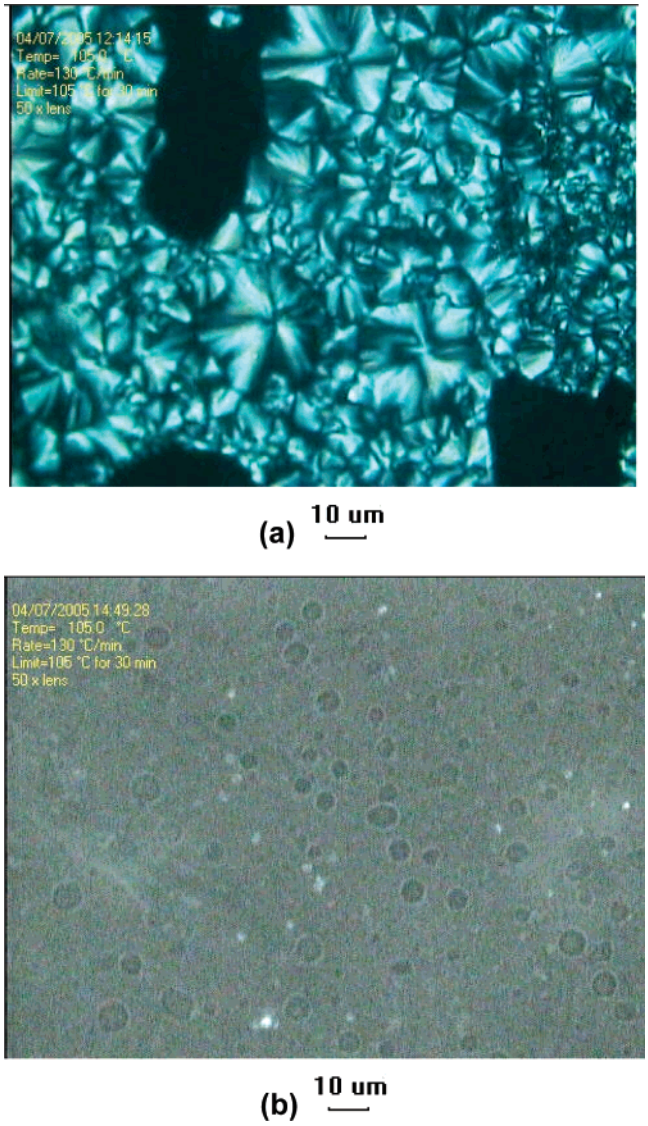

Figure 9. Spherulitic morphologies after 1-min isothermal crystallization at 105 °C for the samples bearing different architectures: (a) **R2**; (b) **S2**.

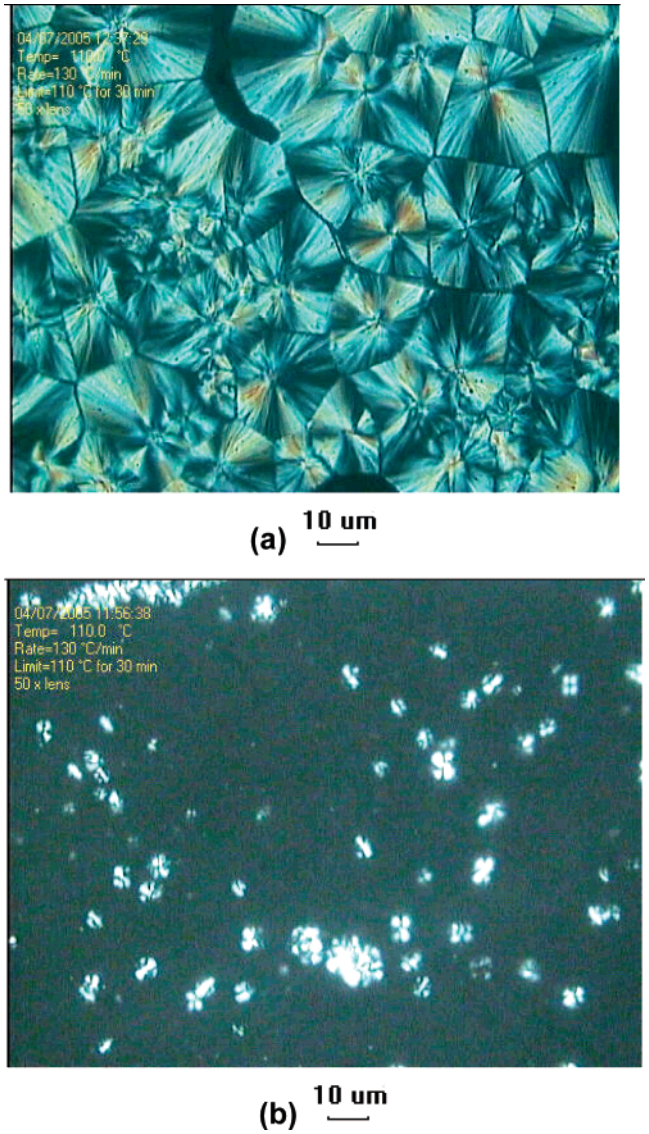

Figure 10. Spherulitic morphologies after 1-min isothermal crystallization at 110 °C for the samples bearing different architectures: (a) **R3**; (b) **S3**.

thermal stability; therefore, the weight fraction of each component was evaluated by TGA as shown in Table 1, indicating good agreement with the calculated results by NMR. In a view of thermal degradation temperatures (T_d) as seen in Table 2, a longer PLLA block of linear diblock MPEG-*b*-PLLA or a less-armed structure of new MPEG-*b*-$(PLLA)_n$ would lead to a higher thermal degradation temperature, and the lower thermal stabilities of new AB_n-shaped diblock copolymers could be accounted for by more active terminal functional groups which could accelerate the chain-end-initiated PLLA thermal degradation.

Spherulitic Morphologies of New AB_n-Shaped Semicrystalline Amphiphilic MPEG-*b*-$(PLLA)_n$. Until now, there have been a number of articles in the literature on crystal morphologies of biodegradable PLLA bearing diverse molecular architectures as well as diblock MPEG-*b*-PLLA.[38,50−51] Here, Figure 8 depicts spherulite morphologies after 1-min isothermal crystallization at a given temperature of 105 °C for the linear MPEG-*b*-PLLA **R1** (a) and new Y-shaped MPEG-*b*-$(PLLA)_2$ **S1** (b). A larger number of tiny crystal nuclei immediately occurred after 1-min isothermal crystallization at 105 °C, indicating a very fast nucleation rate for the linear **R1** bearing similar weight fractions of the MPEG and PLLA blocks. In contrast, very few

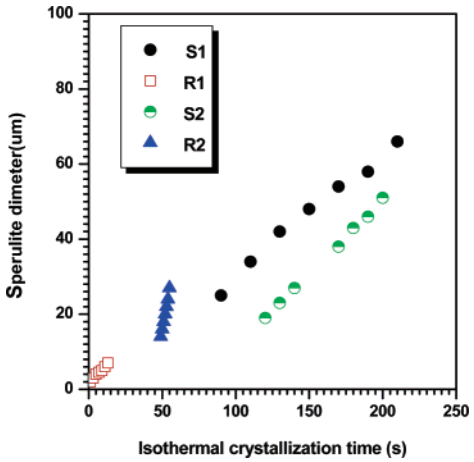

Figure 11. Isothermal crystallization time dependence of spherulite diameters at 105 °C for the synthesized copolymers **R1**, **R2**, **S1**, and **S2**.

crystal nuclei could be observed for the Y-shaped MPEG-*b*-$(PLLA)_2$ **S1**, demonstrating that the multiarmed molecular architecture significantly depressed the crystallizability of PLLA

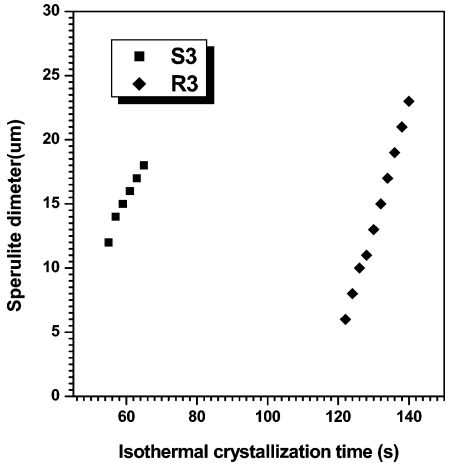

Figure 12. Isothermal crystallization time dependence of spherulite diameters at 110 °C for the synthesized copolymers **R3** and **S3**.

segments. Furthermore, spherulite morphologies after 1-min isothermal crystallization at 105 °C were also shown in Figure 9 for the linear diblock MPEG-*b*-PLLA **R2** (a) and new asymmetric AB_4-shaped MPEG-*b*-$(PLLA)_4$ **S2** (b). During 1-min isothermal crystallization, both tiny and large-sized spherulites concurrently occurred and rapidly impinged with each other for the linear **R2**, exhibiting a spherulite texture much different from that of the **R1** with shorter PLLA block length, while there were few detectable crystal nuclei for the AB_4-shaped MPEG-*b*-$(PLLA)_4$ **S2** even though it has a similar PLLA weight fraction (more than 70 wt %). In addition, at an increased temperature of 110 °C, large and rapidly impinged spherulites after 1-min isothermal crystallization were shown in Figure 10 for the linear MPEG-*b*-PLLA **R3** (a). With increasing isothermal crystallization temperature, the diblock MPEG-*b*-PLLA **R3** bearing a greatly extended PLLA block tended to organize low-density crystal nuclei and large-sized spherulites in a rapid crystal growth way. In the meantime, new asymmetric AB_8-shaped MPEG-*b*-$(PLLA)_8$ **S3** only showed a small number of tiny crystal nuclei, regardless of its PLLA component weight fraction higher than 88 wt %.

Figures 11 and 12 depict the spherulite diameters as a function of isothermal crystallization time at corresponding crystallization temperatures of 105 and 110 °C for the linear MPEG-*b*-PLLA and new AB_n-shaped MPEG-*b*-$(PLLA)_n$, respectively, and good linear relationships were apparently detected. Furthermore, the spherulite growth rates at 105 °C were evaluated to be 0.20 and 0.16 μm s^{-1} for the **R1** and **S1**, respectively, indicating a decreased spherulite growth rate for the multiple-armed **S1**. Similarly, under the same isothermal crystallization temperature, the **R2** and **S2** showed spherulite growth rates equal to 1.05 and 0.20 μm s^{-1}, respectively, implying a more obviously depressed crystallization rate for the **S2**, and different spherulite growth rates of 0.47 and 0.29 μm s^{-1} were respectively evaluated for the **R3** and **S3** under an increased crystallization temperature T_c of 110 °C. In addition, it was also found that after a long isothermal crystallization time much different well-developed spherulite textures appeared as shown in Figure 13,

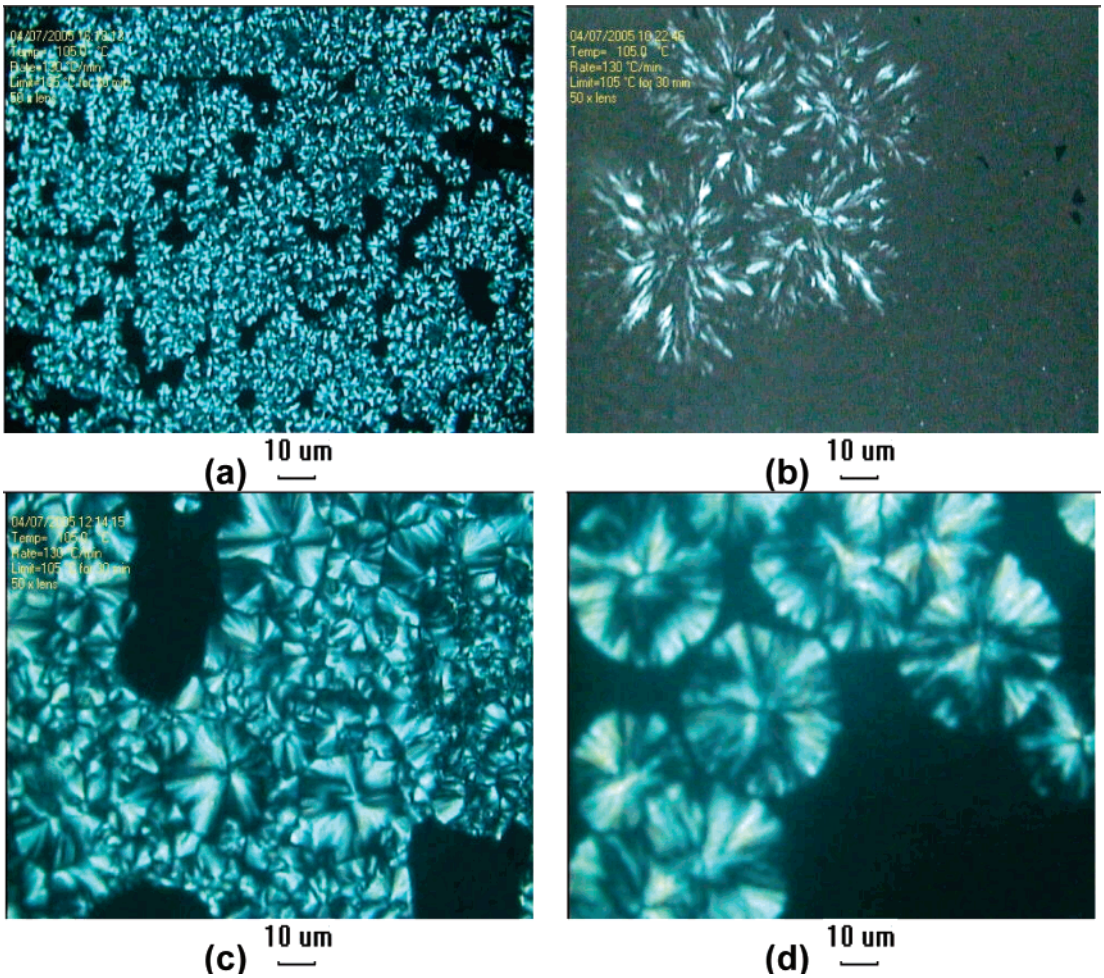

Figure 13. Developed spherulitic morphologies for the isothermally crystallized AB_n-shaped samples as well as linear structural references at 105 °C: (a) **R1**; (b) **S1**; (c) **R2**; (d) **S2**.

i.e., the linear structural **R1** eventually showed tiny spherulites with a high density of crystal nuclei, and impinged spherulites with greatly increased sizes could be found for the sample **R2** with extended PLLA block length. In contrast, the new MPEG-*b*-$(PLLA)_2$ **S1** finally exhibited an interesting coarse spherulitic texture with a large amount of amorphous components entrapped, and relatively large-sized spherulites were observed for the MPEG-*b*-$(PLLA)_4$ **S2**. On this evidence, the AB_n-shaped molecular architecture could therefore be concluded to significantly influence the crystallization kinetics and spherulite morphologies.

Conclusions

In this work, a new series of asymmetric AB_n-shaped amphiphilic biodegradable diblock methoxy poly(ethylene glycol)-*b*-[poly(L-lactide)]$_n$ MPEG-*b*-$(PLLA)_n$ ($n = 2, 4, 8$) have been rationally designed and successfully synthesized with corresponding dendritic Bis-HMPA linkages **L1**−**L3**. At first, new hydroxy end-capped functional MPEG-$(OH)_n$ macroinitiators were derived from a starting monofunctional MPEG-2K and Bis-HMPA via ester coupling and a facile hydroxy protection−deprotection cycle, and chemical structures of these prepared hydroxy-terminated macroinitiators were further characterized by NMR and MALDI−FTMS. The new occurrence of ester bonds and MALDI−FTMS signals demonstrated successful preparation of the A-$(OH)_n$ ($n = 2, 4, 8$)-shaped macroinitiators. Subsequently, novel asymmetric AB_n-shaped amphiphilic diblock MPEG-*b*-$(PLLA)_2$ **S1**, MPEG-*b*-$(PLLA)_4$ **S2**, and MPEG-*b*-$(PLLA)_8$ **S3** bearing similar PLLA arm weight close to 2 KDa as well as linear diblock MPEG-*b*-PLLA (**R1**−**R3**) were synthesized through ring-opening polymerization of L-lactide with corresponding macroinitiators at 130 °C in *m*-xylene. GPC results indicated that either the prepared macroinitiator or a new AB_n-shaped amphiphilic diblock MPEG-*b*-$(PLLA)_n$ exhibited narrow molecular weight distribution, demonstrating its well-defined structure. Furthermore, regarding the molecular architecture dependence of crystallization behavior and spherulite morphologies, thermal analysis of these new AB_n-shaped MPEG-*b*-$(PLLA)_n$ showed greatly depressed crystallizabilities and less-ordered crystal structures as compared to their linear structural references. In addition, the spherulite morphologies studied by POM showed interesting textures so that at a given crystallization temperature of 105 °C very few crystal nuclei could be detected for the new AB_n-shaped MPEG-*b*-$(PLLA)_2$ **S1** and MPEG-*b*-$(PLLA)_4$ **S2** after 1-min isothermal crystallization. In contrast, a high density of PLLA crystal nuclei were found for the linear diblock MPEG-*b*-PLLA **R1**, and the longer PLLA block of a linear diblock MPEG-*b*-PLLA eventually led to larger-sized spherulites in a rapid crystal growth way. Moreover, after a long isothermal crystallization time, very coarse spherulite morphologies were detected for the new AB_n-shaped MPEG-*b*-$(PLLA)_n$ bearing multiple arms.

Furthermore, new investigations on the crystallization kinetics and macromolecular assembly on solid substrate and in solution and their possible applications as novel potential biomaterials are now ongoing in this lab.

Acknowledgment. The authors are grateful to the important fund supports partially from the National Science Foundation of China (20204019, 20574087) and Rising Star and Nanotechnology projects (04QMX1445 and 0452 nm050) of Science and Technology Committee of Shanghai Municipality (STCSM).

References and Notes

(1) Ramzi, A.; Prager, M.; Richter, D.; Efstratiadis, V.; Hadjichristidis, N.; Young, R. N.; Allgaier, J. B. *Macromolecules* **1997**, *30*, 7171.
(2) Pispas, S.; Hadjichristidis, N.; Potemkin, I.; Khokhlov, A. *Macromolecules* **2000**, *33*, 1741.
(3) (a) Ishizu, K.; Uchida, S. *Prog. Polym. Sci.* **1999**, *24*, 1439. (b) Hadjichristidis, N. *J. Polym. Sci., Part A: Polym. Chem.* **1999**, *37*, 857. (c) Hadjichristidis, N.; Pitsikalis, M.; Pispas, S.; Iatrou, H. *Chem. Rev.* **2001**, *101*, 3747. (d) Iatrou, H.; Hadjichristidis, N. *Macromolecules* **1992**, *25*, 4649.
(4) Hadjichristidis, N.; Pispas, S.; Pitsikalis, M.; Iatrou, H.; Vlahos, C. *Adv. Polym. Sci.* **1999**, *142*, 71.
(5) Yamauchi, K.; Takahashi, K.; Hasegawa, H.; Iatrou, H.; Hadjichristidis, N.; Kaneko, T.; Nishikawa, Y.; Jinnai, H.; Matsui, T.; Nishioka, H.; Shimizu, M.; Furukawa, H. *Macromolecules* **2003**, *36*, 6962.
(6) Hückstädt, H.; Göpfert, A.; Abetz, V. *Macromol. Chem. Phys.* **2000**, *201*, 296.
(7) (a) Avgeropoulos, A.; Dair, B. J.; Thomas, E. L.; Hadjichristidis, N. *Polymer* **2002**, *43*, 3257. (b) Zioga, A.; Sioula, S.; Hadjichristidis, N. *Macromol. Symp.* **2000**, *157*, 239.
(8) Hadjichristidis, N.; Iatrou, H.; Pispas, S.; Pitsikalis, M. *J. Polym. Sci., Part A: Polym. Chem.* **2000**, *38*, 3211.
(9) Reutenauer, S.; Hurtrez, G.; Dumas, P. *Macromolecules* **2001**, *34*, 755
(10) Pitsikalis, M.; Pispas, S.; Mays, J. W.; Hadjichristidis, N. *Adv. Polym. Sci.* **1998**, *135*, 1.
(11) Hawker, C. J. *Adv. Polym. Sci.* **1999**, *147*, 113.
(12) Hadjichristidis, N.; Pispas, S.; Pitsikalis, M.; Iatrou, H.; Vlahos, C. *Adv. Polym. Sci.* **1999**, *142*, 71.
(13) Gibanel, S.; Forcada, J.; Heroguez, V.; Schappacher, M.; Gnanou, Y. *Macromolecules* **2001**, *34*, 4451.
(14) He, T.; Li, D.; Sheng, X.; Zhao, B. *Macromolecules* **2004**, *37*, 3128.
(15) Cai, Y.; Tang, Y.; Armes, S. P. *Macromolecules* **2004**, *37*, 9728.
(16) Cai, Y.; Armes, S. P. *Macromolecules* **2005**, *38*, 271.
(17) Francis, R.; Lepoittevin, B.; Taton, D.; Gnanou, Y. *Macromolecules* **2002**, *35*, 9001.
(18) Babin, J.; Leroy, C.; Lecommandoux, S.; Borsali, R.; Gnanou, Y.; Taton, D. *Chem. Commun.* **2005**, *38*, 1993.
(19) Milner, S. T. *Macromolecules* **1994**, *27*, 2333.
(20) Olmsted, P. D.; Milner, S. T. *Macromolecules* **1998**, *31*, 4011.
(21) (a) Hadjichristidis, N.; Iatrou, H.; Behal, S. K.; Chludzinski, J. J.; Disko, M. M.; Garner, R. T.; Liang, K. S.; Lohse, D. J.; Milner, S. T. *Macromolecules* **1993**, *26*, 5812. (b) Pochan, D. J.; Gido, S. P.; Pispas, S.; Mays, J. W.; Ryan, A. J.; Fairclough, J. P. A.; Hamley, I. W.; Terrill, N. *Macromolecules* **1996**, *29*, 5091.
(22) Tselikas, Y.; Iatrou, H.; Hadjichristidis, N.; Liang, K. S.; Lohse, D. J. *J. Chem. Phys.* **1996**, *105*, 2456.
(23) Beyer, F. L.; Gido, S. P.; Velis, G.; Hadjichristidis, N.; Tan, N. B. *Macromolecules* **1999**, *32*, 6604.
(24) (a) Beyer, F. L.; Gido, S. P.; Poulos, Y.; Avgeropoulos, A.; Hadjichristidis, N. *Macromolecules* **1997**, *30*, 2373. (b) Turner, C. M.; Sheller, N. B.; Foster, M. D.; Lee, B.; Corona-Galvin, S.; Quirk, R. P.; Annis, B.; Lin, J. S. *Macromolecules* **1998**, *31*, 4372.
(25) Sotiriou, K.; Nannou, A.; Velis, G.; Pispas, S. *Macromolecules* **2002**, *35*, 4106.
(26) Peleshanko, S.; Jeong, J.; Shevchenko, V. V.; Genson, K. L.; Pikus, Y.; Ornatska, M.; Petrash, S.; Tsukruk, V. V. *Macromolecules* **2004**, *37*, 7497.
(27) Peleshanko, S.; Jeong, J.; Gunawidjaja, R.; Tsukruk, V. V. *Macromolecules* **2004**, *37*, 6511.
(28) Peleshanko, S.; Gunawidjaja, R.; Jeong, J.; Shevchenko, V. V.; Tsukruk, V. V. *Langmuir* **2004**, *20*, 9423.
(29) Okada, M. *Prog. Polym. Sci.* **2002**, *27*, 87.
(30) Uhrich, K. E.; Cannizzaro, S. M.; Langer, R. S.; Shakesheff, K. M. *Chem. Rev.* **1999**, *99*, 3181.
(31) Jeong, B. M.; Bae, Y. H.; Lee, D. S.; Kim, S. W. *Nature (London)* **1997**, *388*, 860.
(32) Robert, L. *Science* **1993**, *260*, 920.
(33) Chiellini, E.; Solaro, R. *Adv. Mater.* **1996**, *8*, 305.
(34) Herold, D. A.; Keil, K.; Bruns, D. E. *Biochem. Pharmacol.* **1989**, *38*, 73.
(35) (a) Aamer, K. A.; Sardinha, H.; Bhatia, S. R.; Tew, G. N. *Biomaterials* **2004**, *25*, 1087. (b) Du, Y. J.; Lemstra, P. J.; Nijenhuis, A. J.; Aert, H. A. M. V.; Bastiaansen, C. *Macromolecules* **1995**, *28*, 2124.

(36) (a) Shin, D.; Shin, K.; Aamer, K. A.; Tew, G. N.; Russell, T. P.; Lee, J. H.; Jho, J. Y. *Macromolecules* **2005**, *38*, 104. (b) Lee, S. Y.; Chin, I. J.; Jung, J. S. *Eur. Polym. J.* **1999**, *35*, 2147. (c) Kim, K.-S.; Chung, S.; Chin, I. J.; Kim, M. N.; Yoon, J. S. *J. Appl. Polym. Sci.* **1999**, *72*, 341. (d) Sun, J.; Hong, Z.; Yang, L.; Tang, Z.; Chen, X.; Jing, X. *Polymer* **2004**, *45*, 5969.
(37) (a) Fujiwara, T.; Miyamoto, M.; Kimura, Y.; Iwata, T.; Doi, Y. *Macromolecules* **2001**, *34*, 4043. (b) Slager, J.; Domb, A. J. *Biomacromolecules* **2003**, *4*, 1308. (c) Lucke, A.; Tessmar, J.; Schnell, E.; Schmeer, G.; Göpferich, A. *Biomaterials* **2000**, *21*, 2361. (d) De Jong, S. J.; De Smedt, S. C.; Wahls, M. W. C.; Demeester, J.; Kettenes-van den Bosch, J. J.; Hennink, W. E. *Macromolecules* **2000**, *33*, 3680. (e) Frick, E. M.; Zalusky, A. S.; Hillmyer, M. A. *Biomacromolecules* **2003**, *4*, 216.
(38) Hao, Q.; Li, F.; Li, Q.; Li, Y.; Jia, L.; Yang, J.; Fang, Q.; Cao, A.; *Biomacromolecules* **2005**, *6*, 2236.
(39) Hecht, S.; Vladimirov, N.; Fréchet, J. M. J. *J. Am. Chem. Soc.* **2001**, *123*, 18.
(40) Michael, M.; Eva, M.; Anders, H. *Macromolecules* **2002**, *35*, 8307.
(41) Chapman, T. M.; Hillyer, G. L.; Mahan, E. J.; Shaffer, K. A. *J. Am. Chem. Soc.* **1994**, *116*, 11195.
(42) Ihre, H.; Hult, A.; Soderlind, E. *J. Am. Chem. Soc.* **1996**, *118*, 6388.
(43) Ihre, H.; Hult, A.; Fréchet, J. M. J.; Gitsov, I. *Macromolecules* **1998**, *31*, 4061.
(44) Moore, J. S.; Stupp, S. I. *Macromolecules* **1990**, *23*, 65.
(45) Ihre, H.; Padilla De Jesus, O. L.; Fréchet, J. M. J. *J. Am. Chem. Soc.* **2001**, *123*, 5908.
(46) Ling, F. H.; Lu, V.; Svec, F.; Fréchet, J. M. J. *J. Org. Chem.* **2002**, *67*, 1993.
(47) Hecht S.; Ihre H.; Fréchet, J. M. J. *J. Am. Chem. Soc.* **1999**, *121*, 9239.
(48) O'Keefe, B. J.; Hillmyer, M. A.; Tolman, W. B. *J. Chem. Soc., Dalton Trans.* **2001**, *2215*.
(49) Bogdanov, B.; Vidts, A.; Buicke, A. V. D.; Verbeeck, R.; Schacht, E. *Polymer* **1998**, *39*, 1631.
(50) Tsuji, H.; Miyase, T.; Tezuka, Y.; Saha, S. K. *Biomacromolecules* **2005**, *6*, 244.
(51) Sun, J.; Zhuang, X.; Chen, X.; Jing, X. *Chem. J. Chin. Univ.* **2005**, *26*, 956.
(52) Abe, H.; Doi, Y.; Aoki, H.; Akehata, T. *Macromolecules* **1998**, *31*, 1791.
(53) Kowalski, A.; Duda, A.; Penczek, S. *Macromolecules* **2000**, 33, 689.

BM060372L